Original Article

Institution of MECHANICAL ENGINEERS
Journal of AUTOMOBILE ENGINEERING

Proc IMechE Part D:
J Automobile Engineering
226(6) 779–794

DOI: 10.1177/0954407011430919
pid.sagepub.com
SAGE

A robust road bank angle estimation based on a proportional–integral H_∞ filter

Jihwan Kim[1], Hyeongcheol Lee[1] and Seibum Choi[2]

Abstract

This paper presents a new robust road bank angle estimation method that does not require a differential global positioning system or any additional expensive sensors. A modified bicycle model, which is less sensitive to model uncertainties than is the conventional bicycle model, is proposed. The road bank angle estimation algorithm designed using this model can improve robustness against modelling errors and uncertainties. A proportional–integral H_∞ filter based on the game theory approach, which is designed for the worst cases with respect to the sensor noises and disturbances, is used as the estimator in order to improve further the stability and robustness of the bank estimation. The effectiveness and performance of the proposed estimation algorithm are verified by simulations and tests, and the results are compared with those of previous road bank angle estimation methods.

Keywords

Road bank angle estimation, proportional–integral H_∞ filter, modified bicycle model, observer-based disturbance estimation

Date received: 24 January 2011; accepted: 14 October 2011

Introduction

Various vehicle chassis control systems have been developed for modern automobiles to meet increased performance and safety requirements.[1–7] Since the road variables, such as the slipperiness, roughness, grade angle and bank angle, directly affect the vehicle dynamics, vehicle chassis control systems can benefit significantly by using information about the road variables in real applications, in terms of improved control accuracy, robustness and environmental adaptiveness.

Among the road variables, the road bank angle has a direct influence on the lateral and roll dynamics of the vehicle. Therefore, estimation of the road bank angle has been a significant research topic for vehicle stability control,[8,9] rollover prevention[10–12] and fault management.[12,13] The availability of accurate road bank angle information not only improves the accuracy of lateral speed estimation, which in turn improves the accuracy of stability control,[1,2,8,9] but also prevents unnecessary activation of vehicle stability control systems when the vehicle is on a banked road.[2,8] Road bank angle estimation is an essential part of vehicle rollover prevention systems, because significant road bank angles can create different vehicle roll behaviours during the transient manoeuvring in which most rollover accidents actually occur.[10,12] Road bank angle estimation is also necessary for model-based sensor fault detection.[12,13]

The road bank angle is difficult to measure directly with commercially available sensors, because it is often coupled with other vehicle dynamics in sensor measurements, such as the lateral acceleration and the roll and pitch angles of the vehicle. For example, the lateral accelerometer measurement includes not only the acceleration of gravity due to the road bank angle but also the lateral acceleration.[8] In other words, it is difficult to distinguish driving on a banked road from cornering on a flat low-μ surface, by using only the lateral accelerometer measurement.

Several studies have been conducted to explore the estimation of the road bank angle. The road bank

[1]Department of Electrical and Biomedical Engineering, Hanyang University, Seoul, Republic of Korea
[2]Department of Mechanical Engineering, Korea Advanced Institute of Science and Technology, Daejeon, Republic of Korea

Corresponding author:
Hyeongcheol Lee, Department of Electrical and Biomedical Engineering, Hanyang University, Seoul 133-791, Republic of Korea.
Email: hclee@hanyang.ac.kr

angle and modelling errors are defined as uncertain parameters and they are estimated using a disturbance observer[10] and the adaptive control theory.[14] These estimation methods require the side-slip angle, which can be estimated using the differential global positioning system (DGPS) measurement. Different from the one-antenna global positioning system (GPS), which is generally used in automotive navigation systems, the DGPS with two antennae is too expensive to be used in passenger cars and is frequently unreliable in urban environments.[9] Even though these methods can guarantee an acceptable accuracy of estimation, they are not practical solutions owing to the cost and reliability issues related to the DGPS. A road bank angle estimation using a vertical accelerometer is proposed.[9] However, the vertical accelerometer measurement also cannot provide an acceptable accuracy of the road bank angle because the vertical accelerometer is almost insensitive to the narrow range of vehicle tilts owing to the non-linearity of the arccosine functional relation between the vertical acceleration and the vehicle tilt.[15]

The road bank angle has been estimated using the differences between the lateral tyre force estimate and the lateral accelerometer measurement,[16] or the differences between the lateral acceleration measurement and the products of the yaw rate and the longitudinal speed[17] in the linear observer framework. However, these methods tend to be inaccurate under transient driving conditions because they neglect the derivative term of the lateral velocity of the vehicle. A road bank angle estimation method based on the transfer function and dynamic filter compensation (DFC), which is related to the model uncertainty of the lateral dynamics, was previously introduced.[8,12] This method illustrated the robustness issues of the road bank angle estimation; however, the physical meaning of the DFC term was not explicitly explained in the papers.

Disturbance observers based on the unknown input observer (UIO), which is a well-known solution for the state and disturbance estimation of linear systems, were proposed to estimate the road bank angle.[13,18] This method can guarantee the stability and convergence of the estimation error, but estimation by this method is sensitive to the output changes because of the derivative term of the output in the observer. More complex methods that consider the roll dynamics of vehicles[19,20] were developed in order to estimate the roll angle of the vehicle and the road bank angle individually. On the other hand, non-linear modelling and table-based estimation methods[21] were developed in order to improve the accuracy of the state estimation of the lateral dynamics. However, most of the previous road bank angle estimation methods explained above did not address the robustness issue of the estimation due to uncertainties and disturbances, such as the cornering stiffnesses of the tyres and the changes in the vehicle mass.

This paper presents a new robust road bank angle estimation method that does not require DGPS or any additional expensive sensors. A modified bicycle model, which is less sensitive to model uncertainties such as the cornering stiffnesses of the tyres than is the conventional bicycle model, is proposed in this paper. Therefore, the road bank angle estimation algorithm designed using this model can be more robust against modelling errors and uncertainties than using the conventional bicycle model. A proportional–integral H_∞ filter (PIF) based on the game theory approach, which is designed for the worst cases with respect to the sensor noises and disturbances, is used as the estimator in order to improve further the stability and robustness of the bank estimation. The effectiveness and performance of the proposed estimation algorithm are verified by simulations and tests, and the results are compared with those of previous road bank angle estimation methods.

Vehicle dynamics model

Figure 1 shows the schematic diagrams of the target system. As shown in Figure 1(a), by assuming the bicycle model (i.e. by assuming that the dynamics of the left and right sides of the vehicle are identical) and no pitch motion, the lateral motion of the vehicle[22,23] can be expressed by

$$\begin{aligned} ma_y &= F_{yf} + F_{yr} \\ I_z\ddot{\psi} &= L_f F_{yf} - L_r F_{yr} \end{aligned} \tag{1}$$

The lateral accelerometer measurement consists of three components, namely the linear motion term, the lateral motion term and the gravity term, according to[22]

$$a_y = \dot{v}_y + v_x\dot{\psi} + g\sin(\phi_b + \phi) \tag{2}$$

where ϕ_b is the road bank angle and ϕ is the roll angle of the vehicle. By equation (2), it is shown that the lateral acceleration measurement includes not only the dynamic component $\dot{v}_y + v_x r$ of the vehicle motion but also the gravity component $g\sin(\phi_b + \phi)$ of the road bank angle and the roll angle. By assuming that the lateral forces of the tyres are linearly proportional to the cornering stiffnesses of the tyres and that the slip angles of the tyres are very small, the lateral force of each tyre can be expressed as[22,23]

$$\begin{aligned} F_{yf} &\approx -C_f\alpha_f = -C_f(\beta_f - \delta_f) \\ F_{yr} &\approx -C_r\alpha_r = -C_r\beta_r \\ \beta_f &= \tan^{-1}\left(\frac{v_y + L_f\dot{\psi}}{v_x}\right) \approx \frac{v_y + L_f\dot{\psi}}{v_x} \\ \beta_r &= \tan^{-1}\left(\frac{v_y - L_r\dot{\psi}}{v_x}\right) \approx \frac{v_y - L_r\dot{\psi}}{v_x} \\ C_f &= \left.\frac{\partial F_{yf}}{\partial\alpha_f}\right|_{\alpha_f = 0}, \quad C_r = \left.\frac{\partial F_{yr}}{\partial\alpha_r}\right|_{\alpha_r = 0} \end{aligned} \tag{3}$$

For simplification, let $\varphi = \phi_b + \phi$. From equations (1), (2) and (3), the lateral and yaw motions of a vehicle are expressed by the state equations

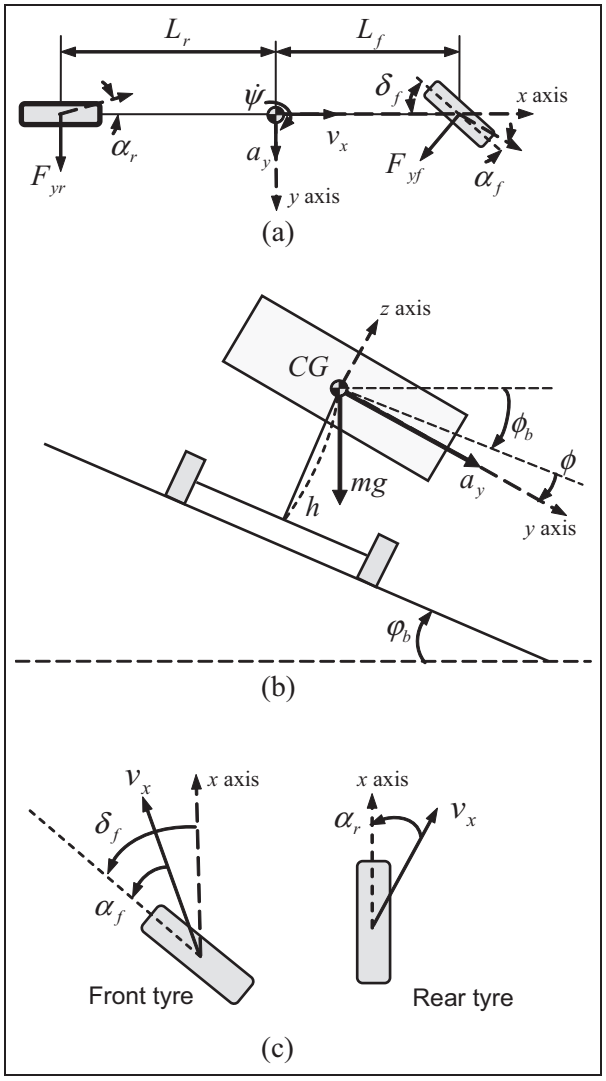

Figure 1. Schematic diagrams of the target system: (a) bicycle model of a vehicle; (b) rear view of a vehicle; (c) tyre diagram. CG: centre of gravity.

$$\dot{x} = A_o x + B_o u_o + E_o w$$
$$y_o = C_o x + D_o u_o \tag{4}$$

where

$$x = \begin{pmatrix} v_y \\ \dot{\psi} \end{pmatrix}, \quad y_o = \begin{pmatrix} a_y \\ \dot{\psi} \end{pmatrix}$$
$$u_o = \delta_f, \quad w = \sin\varphi$$
$$A_o = \begin{pmatrix} -\frac{C_f + C_r}{mv_x} & -\frac{L_f C_f - L_r C_r}{mv_x} - v_x \\ -\frac{L_f C_f - L_r C_r}{I_z v_x} & -\frac{L_f^2 C_f + L_r^2 C_r}{I_z v_x} \end{pmatrix}$$
$$B_o = \begin{pmatrix} \frac{C_f}{m} \\ \frac{L_f C_f}{I_z} \end{pmatrix}$$
$$C_o = \begin{pmatrix} -\frac{C_f + C_r}{mv_x} & -\frac{L_f C_f - L_r C_r}{mv_x} \\ 0 & 1 \end{pmatrix}$$
$$D_o = \begin{pmatrix} \frac{C_f}{m} \\ 0 \end{pmatrix}, \quad E_o = \begin{pmatrix} -g \\ 0 \end{pmatrix}$$

The mathematical model expressed by equations (4) does not fully agree with the actual system owing to the inevitable model uncertainties. Specifically, the modelling error in the cornering stiffnesses C_f and C_r, which results from the linear lateral force assumption and the small-side-slip-angle assumption, is one of the major causes of the model uncertainties. Moreover, the lateral forces of the front tyres of a front-wheel-drive vehicle are affected not only by the side-slip angles but also by the traction forces. Therefore, the cornering stiffness of the front tyres of a front-wheel-drive vehicle may incur more model inaccuracies than that of the rear tyres during the traction. A modified vehicle model describing more accurate vehicle lateral and yaw motions can be obtained by eliminating the cornering stiffness terms of the front tyres from the vehicle's lateral equations of motion. From equation (2) and the second equation of equation (1), the equations which do not include the F_{yf} term can be obtained as

$$\dot{v}_y = a_y - v_x\dot{\psi} - g\sin\varphi$$
$$I_z\ddot{\psi} = L_f m a_y - (L_f + L_r)F_{yr} \tag{5}$$

From equations (5) and (3), the state equations of the modified vehicle dynamic model can be obtained as

$$\dot{x} = A_m x + B_m u_m + E_m w$$
$$y_m = C_m x \tag{6}$$

where

$$x = \begin{pmatrix} v_y \\ \dot{\psi} \end{pmatrix}, \quad u_m = a_y, \quad w = \sin\varphi$$
$$A_m = \begin{pmatrix} 0 & -v_x \\ \frac{(L_f + L_r)C_r}{I_z v_x} & -\frac{(L_f + L_r)L_r C_r}{I_z v_x} \end{pmatrix}$$
$$B_m = \begin{pmatrix} 1 \\ \frac{L_f m}{I_z} \end{pmatrix}$$
$$C_m = \begin{pmatrix} 0 & 1 \end{pmatrix}, \quad E_m = \begin{pmatrix} -g \\ 0 \end{pmatrix}$$

As shown in equations (6), the modified model is not affected by the cornering stiffness of the front tyres. Therefore, it can be said that the modified model is less sensitive to variations in the cornering stiffnesses of the tyres than is the conventional bicycle model, and the road bank angle estimation designed using the modified model can be more robust against the uncertainties. Similar analyses can be conducted for rear-wheel-drive vehicles by eliminating the cornering stiffness terms of the rear tyres from the equations of motion of the vehicle.

Robustness analysis of the estimation methods

As commented in the previous section, variations in the cornering stiffnesses of the tyres exist under real driving conditions and they make the parameters of the vehicle model uncertain. For this reason, the effects of the parameter uncertainties on the estimation errors should

be analysed in order to improve the robustness of the estimation.

In this section, four estimation methods derived from equations (4) or equations (6) are explained and analysed in order to compare the robustness of the estimation methods against modelling errors and uncertainties and, in particular, the modelling error in the cornering stiffnesses C_f and C_r.

For clarity, the uncertainties in the cornering stiffnesses are denoted ΔC_f and ΔC_r in this paper. The uncertainties in the system matrices of the original vehicle dynamic model (4) can be expressed by using ΔC_f and ΔC_r as

$$\begin{aligned}
\Delta A_o &= \begin{pmatrix} -\frac{\Delta C_f + \Delta C_r}{m v_x} & -\frac{L_f \Delta C_f - L_r \Delta C_r}{m v_x} \\ -\frac{L_f \Delta C_f - L_r \Delta C_r}{I_z v_x} & -\frac{L_f^2 \Delta C_f + L_r^2 \Delta C_r}{I_z v_x} \end{pmatrix} \\
\Delta B_o &= \begin{pmatrix} \frac{\Delta C_f}{m} \\ \frac{L_f \Delta C_f}{I_z} \end{pmatrix} \\
\Delta C_o &= \begin{pmatrix} -\frac{\Delta C_f + \Delta C_r}{m v_x} & -\frac{L_f \Delta C_f - L_r \Delta C_r}{m v_x} \\ 0 & 0 \end{pmatrix} \\
\Delta D_o &= \begin{pmatrix} \frac{\Delta C_f}{m} \\ 0 \end{pmatrix}
\end{aligned} \tag{7}$$

On the other hand, for the modified vehicle dynamic model (6), the uncertainties in the system matrices can be expressed as

$$\begin{aligned}
\Delta A_m &= \begin{pmatrix} 0 & 0 \\ \frac{(L_f + L_r)\Delta C_r}{I_z v_x} & -\frac{(L_f + L_r) L_r \Delta C_r}{I_z v_x} \end{pmatrix} \\
\Delta B_m &= 0 \\
\Delta C_m &= \begin{pmatrix} 0 & 0 \\ 0 & 0 \end{pmatrix} \\
\Delta D_m &= \begin{pmatrix} 0 \\ 0 \end{pmatrix}
\end{aligned} \tag{8}$$

Dynamic filter compensation method

If the derivative of the lateral speed is zero (i.e. $\dot{v}_y = 0$), the road bank angle estimation can be derived from equation (2) as

$$\sin \hat{\varphi}_v = \frac{a_y - v_x \dot{\psi}}{g} \tag{9}$$

Estimating the road bank angle based on equation (9) simplifies the calculation of the estimation, but the estimation becomes more inaccurate as $|\dot{v}_y|$ becomes larger. The DFC method[8] was proposed to relieve this problem by compensating equation (9) with the DFC term, according to

$$\hat{w}_{dfc} = \sin \hat{\varphi}_v \max\left[0,\ 1 - |\mathrm{DFC}| - \left|\frac{\mathrm{d}}{\mathrm{d}t} \sin \hat{\varphi}_v\right|\right] \tag{10}$$

where

$$\begin{aligned}
\mathrm{DFC}(s) &= H_{aw}[\sin \hat{\varphi}_a(s) - \sin \hat{\varphi}_v(s)] \\
&\quad + v_x H_{rw}[\sin \hat{\varphi}_r(s) - \sin \hat{\varphi}_v(s)] \\
\sin \hat{\varphi}_a(s) &= H_{aw}{}^{-1}[A_y(s) - H_{au} U_o(s)] \\
\sin \hat{\varphi}_r(s) &= H_{rw}{}^{-1}[\dot{\Psi}(s) - H_{ru} U_o(s)] \\
\begin{pmatrix} H_{au} \\ H_{ru} \end{pmatrix} &= C_o(sI - A_o)^{-1} B_o + D_o \\
\begin{pmatrix} H_{aw} \\ H_{rw} \end{pmatrix} &= C_o(sI - A_o)^{-1} E_o
\end{aligned}$$

If the model uncertainties do not exist, $A_y(s) = H_{au} U_o(s) + H_{aw} W(s)$ and $\dot{\Psi}(s) = H_{ru} U_o(s) + H_{rw} W(s)$. This yields

$$\begin{aligned}
\mathrm{DFC}(s) &= H_{aw} W(s) + v_x H_{rw} W(s) \\
&\quad - \frac{(H_{aw} + v_x H_{rw})[A_y(s) - v_x \dot{\Psi}(s)]}{g} \\
&= \frac{-(H_{aw} + v_x H_{rw})[-g W(s) + A_y(s) - v_x \dot{\Psi}(s)]}{g} \\
&= \frac{-(H_{aw} + v_x H_{rw}) s V_y(s)}{g}
\end{aligned} \tag{11}$$

In equation (11), $(H_{aw} + v_x H_{rw})/g$ is a form of second-order low-pass filter and therefore DFC can be considered as an estimation of $\dot{v}_y$. If the model uncertainties exist, the transfer functions of equations (4) can be expressed as

$$\begin{aligned}
\begin{pmatrix} \bar{H}_{au} \\ \bar{H}_{ru} \end{pmatrix} &= (C_o + \Delta C_o)(sI - A_o - \Delta A_o)^{-1}(B_o + \Delta B_o) \\
&\quad + D_o + \Delta D_o \\
\begin{pmatrix} \bar{H}_{aw} \\ \bar{H}_{rw} \end{pmatrix} &= (C_o + \Delta C_o)(sI - A_o - \Delta A_o)^{-1} E_o
\end{aligned} \tag{12}$$

Then, the uncertainties in the transfer functions are

$$\begin{aligned}
\Delta H_{au} &= \bar{H}_{au} - H_{au}, \quad \Delta H_{ru} = \bar{H}_{ru} - H_{ru} \\
\Delta H_{aw} &= \bar{H}_{aw} - H_{aw}, \quad \Delta H_{rw} = \bar{H}_{rw} - H_{rw}
\end{aligned} \tag{13}$$

In this case, the DFC can be obtained as

$$\begin{aligned}
\mathrm{DFC}(s) &= H_{aw} W(s) + v_x H_{rw} W(s) \\
&\quad - \frac{(H_{aw} + v_x H_{rw})[A_y(s) - v_x \dot{\Psi}(s)]}{g} \\
&\quad + \Delta H_{au}\, U_o(s) + \Delta H_{aw}\, W(s) + v_x\, \Delta H_{ru}\, U_o(s) \\
&\quad + v_x\, \Delta H_{rw}\, W(s) \\
&= \frac{-(H_{aw} + v_x H_{rw}) s V_y(s)}{g} + (\Delta H_{au} + v_x\, \Delta H_{ru}) U_o(s) \\
&\quad + (\Delta H_{aw} + v_x\, \Delta H_{rw}) W(s)
\end{aligned} \tag{14}$$

Equation (14) implies that the model uncertainties make the DFC inaccurate from the viewpoint of the $\dot{v}_y$ estimation because $\Delta H_{au} + v_x \Delta H_{ru}$ and $\Delta H_{aw} + v_x \Delta H_{rw}$

are non-zero even if the system is in a steady state. For this reason, $\hat{w}_{dfc}$ has steady state errors if u_o or w are not zero.

It was proposed by Tseng[8] that the steady state values of the transfer functions H_{aw} and $v_x H_{rw}$ are actually implemented for the actual automotive applications to mitigate the computational burden, according to

$$\begin{aligned}\lim_{s\to 0} H_{aw} &= -\frac{g(L_f + L_r)}{(L_f + L_r) + K_{us} v_x^2} \\ \lim_{s\to 0} v_x H_{rw} &= \frac{g K_{us} v_x^2}{(L_f + L_r) + K_{us} v_x^2}\end{aligned} \tag{15}$$

where

$$K_{us} = \frac{L_r m}{(L_f + L_r) C_f} - \frac{L_f m}{(L_f + L_r) C_r}$$

Unknown input observer method

The UIO is a state observer designed to decouple the state estimation error from the disturbance.[24] The disturbance can be estimated by using the state estimation of the UIO. The form of the UIO[13,18] is expressed by

$$\begin{aligned}\dot{z}_{uio} &= N_{uio} z_{uio} + L_{uio} y_{uio} + G_{uio} u_o \\ \hat{x}_{uio} &= z_{uio} - E_{uio} y_{uio}\end{aligned} \tag{16}$$

where

$$y_{uio} = y_o - D_o u_o$$

N_{uio}, L_{uio}, G_{uio} and E_{uio} can be designed by the following steps. The derivative of $\hat{x}_{uio}$ can be derived from equations (4) and (16) as

$$\begin{aligned}\dot{\hat{x}}_{uio} &= \dot{z}_{uio} - E_{uio} C_o \dot{x} \\ &= N_{uio} z_{uio} + L_{uio} y_o + (G_{uio} - L_{uio} D_o) u_o \\ &\quad - E_{uio} C_o (A_o x + B_o u_o + E_o w)\end{aligned} \tag{17}$$

If the model uncertainties do not exist, the dynamics of the estimation error are given by

$$\begin{aligned}\dot{x} - \dot{\hat{x}}_{uio} &= (I + E_{uio} C_o)(A_o x + B_o u_o + E_o w) - N_{uio} z_{uio} - L_{uio} y_o \\ &\quad - (G_{uio} - L_{uio} D_o) u_o \\ &= [(I + E_{uio} C_o) A_o - M_{uio} C_o](x - \hat{x}_{uio}) + M_{uio} C_o x \\ &\quad + [(I + E_{uio} C_o) A_o - M_{uio} C_o] \hat{x}_{uio} + (I + E_{uio} C_o) B_o u_o \\ &\quad + (I + E_{uio} C_o) E_o w - N_{uio} z_{uio} - L_{uio} y_o - (G_{uio} - L_{uio} D_o) u_o \\ &= [(I + E_{uio} C_o) A_o - M_{uio} C_o](x - \hat{x}_{uio}) \\ &\quad + [(I + E_{uio} C_o) A_o - M_{uio} C_o - N_{uio}] z_{uio} \\ &\quad + [-(I + E_{uio} C_o) A_o E_{uio} + M_{uio} C_o E_{uio} + M_{uio} - L_{uio}] y_o \\ &\quad + \{[(I + E_{uio} C_o) A_o - M_{uio} C_o] E_{uio} D_o + (L_{uio} - M_{uio}) D_o \\ &\quad + (I + E_{uio} C_o) B_o - G_{uio}\} u_o + (I + E_{uio} C_o) E_o w\end{aligned} \tag{18}$$

where M_{uio} is a constant matrix, which should be selected to make $(I + E_{uio} C_o) A_o - M_{uio} C_o$ stable. In order to make equation (18) asymptotically stable (i.e. $\lim_{t\to\infty}(x - \hat{x}_{uio}) = 0$), the equations that should be valid are

$$\begin{aligned}E_{uio} &= -E_o (C_o E_o)^+ + Q_{uio}[I - C_o E_o (C_o E_o)^+] \\ N_{uio} &= (I + E_{uio} C_o) A_o - M_{uio} C_o \\ L_{uio} &= -N_{uio} E_{uio} + M_{uio} \\ G_{uio} &= (I + E_{uio} C_o) B_o\end{aligned} \tag{19}$$

Q_{uio} is a constant matrix, which consists of design parameters and $(C_o E_o)^+$ is the left inverse of $C_o E_o$ (i.e. $[(C_o E_o)^{\mathrm{T}} C_o E_o]^{-1} (C_o E_o)^{\mathrm{T}}$). The estimation of w based on the UIO was proposed by Imsland et al.[18] as

$$\begin{aligned}\hat{w}_{uio} = E_o^+ [&L_{uio} y_{uio} - E_{uio} \dot{y}_{uio} \\ &-(L_{uio} C_o - E_{uio} C_o A_o) \hat{x}_{uio} + E_{uio} C_o B_o u_o]\end{aligned} \tag{20}$$

If the model uncertainties do not exist,

$$\begin{aligned}E_o(w - \hat{w}_{uio}) &= E_o w - L_{uio} C_o x + E_{uio} C_o (A_o x + B_o u_o + E_o w) \\ &\quad + (L_{uio} C_o - E_{uio} C_o A_o) \hat{x}_{uio} - E_{uio} C_o B_o u_o \\ &= (E_{uio} C_o A_o - L_{uio} C_o)(x - \hat{x}_{uio}) + (I + E_{uio} C_o) E_o w \\ &= (E_{uio} C_o A_o - L_{uio} C_o)(x - \hat{x}_{uio})\end{aligned} \tag{21}$$

This shows that equation (20) was designed to achieve $\lim_{t\to\infty} \hat{w}_{uio} = w$ by using $\lim_{t\to\infty}(x - \hat{x}_{uio}) = 0$ but, if the model uncertainties exist, the derivative of $\hat{x}_{uio}$ is changed to

$$\begin{aligned}\dot{\hat{x}}_{uio} &= \dot{z}_{uio} - E_{uio}(C_o + \Delta C_o)\dot{x} - E_{uio}\, \Delta D_o\, \dot{u}_o \\ &= N_{uio} z_{uio} + L_{uio} y_o + (G_{uio} - L_{uio} D_o) u_o \\ &\quad - E_{uio}(C_o + \Delta C_o)(A_o x + \Delta A_o\, x + B_o u_o \\ &\quad + \Delta B_o u_o + E_o w) - E_{uio}\, \Delta D_o\, \dot{u}_o\end{aligned} \tag{22}$$

Then, the error dynamics of the UIO are given by

$$\begin{aligned}\dot{x} - \dot{\hat{x}}_{uio} &= (I + E_{uio} C_o + E_{uio}\, \Delta C_o)(A_o x + \Delta A_o\, x \\ &\quad + B_o u_o + \Delta B_o u_o + E_o w) \\ &\quad - N_{uio} z_{uio} - L_{uio} y_o - (G_{uio} - L_{uio} D_o) u_o \\ &\quad + E_{uio}\, \Delta D_o\, \dot{u}_o \\ &= N_{uio}(x - \hat{x}_{uio}) + M_{uio} C_o x + N_{uio} \hat{x}_{uio} \\ &\quad - N_{uio} z_{uio} - L_{uio} y_o + L_{uio} D_o u_o \\ &\quad + E_{uio}\, \Delta C_o\, (A_o x + \Delta A_o\, x + B_o u_o + \Delta B_o\, u_o + E_o w) \\ &\quad + (I + E_{uio} C_o)(\Delta A_o\, x + \Delta B_o\, u_o) + E_{uio}\, \Delta D_o\, \dot{u}_o \\ &= N_{uio}(x - \hat{x}_{uio}) + E_{uio}\, \Delta C_o\, E_o w + E_{uio}\, \Delta D_o\, \dot{u}_o \\ &\quad + [(I + E_{uio} C_o)\, \Delta A_o - M_{uio}\, \Delta C_o \\ &\quad + E_{uio}\, \Delta C_o\, (A_o + \Delta A_o)] x \\ &\quad + [(I + E_{uio} C_o)\, \Delta B_o - M_{uio}\, \Delta D_o \\ &\quad + E_{uio}\, \Delta C_o\, (B_o + \Delta B_o)] u_o\end{aligned} \tag{23}$$

This means that $\lim_{t\to\infty}(x - \hat{x}_{uio}) \neq 0$ if the model uncertainties exist. The error of $\hat{w}_{uio}$ is

$$\begin{aligned} E_o(w-\hat{w}_{uio}) &= E_o w - L_{uio}(C_o+\Delta C_o)x - L_{uio}\,\Delta D_o\,u_o \\ &\quad + E_{uio}C_o(A_o x + \Delta A_o\,x + B_o u_o \\ &\quad + \Delta B_o\,u_o + E_o w) \\ &\quad + (L_{uio}C_o - E_{uio}C_o A_o)\hat{x}_{uio} - E_{uio}C_o B_o u_o \\ &= (E_{uio}C_o A_o - L_{uio}C_o)(x-\hat{x}_{uio}) \\ &\quad + (E_{uio}C_o\,\Delta A_o - L_{uio}\,\Delta C_o)x \\ &\quad + (E_{uio}C_o\,\Delta B_o - L_{uio}\,\Delta D_o)u_o \end{aligned} \tag{24}$$

Therefore, it is concluded that the model uncertainties make both $\hat{x}_{uio}$ and $\hat{w}_{uio}$ inaccurate and $\hat{w}_{uio}$ has steady state errors if x or u_o are not zero.

Because differentiating the output amplifies the effect of the sensor noise, a low-pass filter is used in this paper according to

$$\hat{\dot{y}}_{uio}(s) = \frac{s}{\tau_{uio}s+1}y_{uio}(s) \tag{25}$$

where τ_{uio} is the time constant of the filter.

Proportional–integral observer of the original vehicle dynamic model

The proportional–integral observer (PIO) is a state observer designed to reduce the steady state error by using one or more integration terms of the estimation error.[25,26] A PIO can be derived from the original vehicle dynamic model (4) as

$$\begin{aligned} \dot{\hat{x}}_{po} &= A_o\hat{x}_{po} + B_o u_o + K_{po1}(y_o - \hat{y}_o) + E_o\hat{w}_{po} \\ \dot{\hat{w}}_{po} &= K_{po2}(y_o - \hat{y}_o), \quad \hat{y}_o = C_o\hat{x}_{po} + D_o u_o \end{aligned} \tag{26}$$

where K_{po1} and K_{po2} are the observer gain matrices. If the model uncertainties do not exist, the dynamics of the estimation error are given by

$$\begin{aligned} \dot{x} - \dot{\hat{x}}_{po} &= (A_o - K_{po1}C_o)(x-\hat{x}_{pio}) + E_o(w-\hat{w}_{po}) \\ \dot{w} - \dot{\hat{w}}_{po} &= -K_{po2}C_o(x-\hat{x}_{po}) + \dot{w} \end{aligned} \tag{27}$$

This means that K_{po1} and K_{po2} should be selected to make $A_o - K_{po1}C_o$ and $K_{po2}C_o$ stable. If the model uncertainties exist, the error dynamics of the PIO derived from the original model are changed to

$$\begin{aligned} \dot{x} - \dot{\hat{x}}_{po} &= (A_o - K_{po1}C_o)(x-\hat{x}_{po}) + E_o(w-\hat{w}_{po}) \\ &\quad + (\Delta A_o\,x + \Delta B_o\,u_o) - K_{po1}(\Delta C_o\,x + \Delta D_o\,u_o) \\ \dot{w} - \dot{\hat{w}}_{po} &= -K_{po2}C_o(x-\hat{x}_{po}) + \dot{w} - K_{po2}(\Delta C_o\,x \\ &\quad + \Delta D_o\,u_o) \end{aligned} \tag{28}$$

If the time goes to infinity, the error dynamics of the PIO become

$$\begin{aligned} \lim_{t\to\infty}\begin{pmatrix} x-\hat{x}_{po} \\ w-\hat{w}_{po}\end{pmatrix} &= \begin{pmatrix} A_o - K_{po1}C_o & E_o \\ -K_{po2}C_o & 0\end{pmatrix}^{-1} \\ &\quad \times \begin{pmatrix} K_{po1} & -I \\ K_{po2} & 0\end{pmatrix}\begin{pmatrix} \Delta C_o\,x + \Delta D_o\,u_o \\ \Delta A_o\,x + \Delta B_o\,u_o\end{pmatrix} \end{aligned} \tag{29}$$

It is possible to select K_{po1} and K_{po2} to minimize equation (29) at the cost of reducing the freedom of the observer design (e.g. pole placement methods should be modified in order to minimize equation (29)). However, variations in the other vehicle parameters are ignored in equation (29) and they can amplify the steady state error of the estimation even if equation (29) is minimized by the gain selection.

PIO of the modified vehicle dynamic model

A PIO can be derived from the modified vehicle dynamic model (6) according to

$$\begin{aligned} \dot{\hat{x}}_{pm} &= A_m\hat{x}_{pm} + B_m u_m + K_{pm1}(y_m - \hat{y}_m) + E_m\hat{w}_{pm} \\ \dot{\hat{w}}_{pm} &= K_{pm2}(y_m - \hat{y}_m), \quad \hat{y}_m = C_m\hat{x}_{pm} \end{aligned} \tag{30}$$

where K_{pm1} and K_{pm2} are the observer gain matrices. If the model uncertainties exist, the error dynamics of the PIO of the modified model are given by

$$\begin{aligned} \dot{x} - \dot{\hat{x}}_{pm} &= (A_m - K_{pm1}C_m)(x-\hat{x}_{pm}) + E_m(w-\hat{w}_{pm}) + \Delta A_m\,x \\ \dot{w} - \dot{\hat{w}}_{pm} &= -K_{pm2}C_m(x-\hat{x}_{pm}) + \dot{w} \end{aligned} \tag{31}$$

If the time goes to infinity

$$\begin{aligned} \lim_{t\to\infty}(w-\hat{w}_{pm}) &= (\,0 \quad I\,)\begin{pmatrix} A_m - K_{pm1}C_m & E_m \\ -K_{pm2}C_m & 0\end{pmatrix}^{-1} \\ &\quad \times \begin{pmatrix} -\Delta A_m\,x \\ 0\end{pmatrix} = 0 \end{aligned} \tag{32}$$

Therefore, it is concluded that the PIO of the modified model can eliminate the steady state error of $\hat{w}_{pm}$ even if ΔA_m exists. It is notable that the steady state error remains zero even if variations in the other vehicle parameters exist owing to the structure of equations (6).

Proposed road bank angle estimation method

The results of the previous section show that the PIO derived from the modified model is the best solution from the viewpoint of the robust performance of the steady state error. This paper proposes to apply the PIO algorithm to the bank angle estimation using the modified vehicle model (6). By assigning $w = \sin\varphi$ as a new state, equations (6) can be modified as

$$\begin{aligned}\dot{x}_w &= A_w x_w + B_w u_m + E_w n\\ y_m &= C_w x_w + v\\ w &= L_w x_w\end{aligned} \tag{33}$$

where

$$x_w = \begin{pmatrix} v_y \\ \dot{\psi} \\ w \end{pmatrix}, \qquad n = \frac{\mathrm{d}}{\mathrm{d}t}\sin\varphi$$

$$A_w = \begin{pmatrix} 0 & -v_x & -g \\ \frac{(L_f + L_r)C_r}{I_z v_x} & -\frac{(L_f + L_r)L_r C_r}{I_z v_x} & 0 \\ 0 & 0 & 0 \end{pmatrix}$$

$$B_w = \begin{pmatrix} 1 \\ \frac{L_f m}{I_z} \\ 0 \end{pmatrix}, \qquad C_w = \begin{pmatrix} 0 & 1 & 0 \end{pmatrix}$$

$$E_w = \begin{pmatrix} 0 \\ 0 \\ 1 \end{pmatrix}, \qquad L_w = \begin{pmatrix} 0 & 0 & 1 \end{pmatrix}$$

and v is the noise in the yaw rate measurement such as offset and stiction.[27] It is notable that the Luenberger observer derived from equations (33) is the same as the PIO in equations (30).

Because the rank of the observability matrix of the system described by equations (33) is

$$\operatorname{rank}\begin{pmatrix} C_w & C_w A_w & C_w A_w^2 \end{pmatrix}^{\mathrm{T}} = 3 \tag{34}$$

the system described by equation (34) is observable.

In order to make the observer derived from equations (33) robust against a set of disturbances including the disturbance term n and the noise term v, this paper proposes to use a continuous-time H_∞ filter based on the game theory approach.[28–30] The error of the road bank angle estimation is

$$e_w = w - \hat{w} \tag{35}$$

where $\hat{w}$ is the estimation of the road bank angle term. Because the input u_m and the output y_m are the only known terms, the estimate of the road bank angle term should be derived from them. Let

$$\begin{aligned}\hat{w} &= L_w \hat{x}_w\\ \hat{x}_w &= f_{est}(u_m, y_m, \hat{x}_w(0))\end{aligned} \tag{36}$$

where $f_{est}(u_m, y_m, \hat{x}_w(0))$ is the estimation function, which should be determined. From equations (33), (35) and (36), the estimation error at time 0 can be derived as

$$\begin{aligned}e_w(0) &= w(0) - \hat{w}(0)\\ &= L_w[x_w(0) - \hat{x}_w(0)]\end{aligned} \tag{37}$$

On the basis of equations (33), (35), (36) and (37), it can be said that the estimation error e_w is a function of n, v and $x_w(0) - \hat{x}_w(0)$. Therefore, e_w can be expressed as

$$e_w(s) = G_{err}(s)\varepsilon(s) \tag{38}$$

where $\varepsilon = \begin{pmatrix} n & v & x_w(0) - \hat{x}_w(0) \end{pmatrix}^{\mathrm{T}}$. The robustness of the estimation can be achieved by ensuring that $\|e_w\|_\infty$ is less than a certain value.[30] The system ∞-norm of G_{err} is defined as[31]

$$\begin{aligned}\|G_{err}\|_\infty &= \sup_{\varepsilon \neq 0} \sqrt{\frac{\int_0^{t_f} \|e_w\| \,\mathrm{d}t}{\int_0^{t_f} \|\varepsilon\| \,\mathrm{d}t}}\\ &= \sup_{\varepsilon \neq 0} \sqrt{\frac{\int_0^{t_f} (w - \hat{w})^{\mathrm{T}}(w - \hat{w}) \,\mathrm{d}t}{[x_w(0) - \hat{x}_w(0)]^{\mathrm{T}}[x_w(0) - \hat{x}_w(0)] + \int_0^{t_f} (n^{\mathrm{T}} n + v^{\mathrm{T}} v) \,\mathrm{d}t}}\end{aligned} \tag{39}$$

where sup stands for supremum. Because the goal of the H_∞ filter is to make $\|G_{err}\|_\infty$ less than a certain value, the cost function of the H_∞ filter is defined as[28–30]

$$J_w = \frac{\int_0^{t_f} (w - \hat{w})^{\mathrm{T}} S (w - \hat{w}) \,\mathrm{d}t}{[x_w(0) - \hat{x}_w(0)]^{\mathrm{T}} P_0^{-1} [x_w(0) - \hat{x}_w(0)] + \int_0^{t_f} (n^{\mathrm{T}} Q^{-1} n + v^{\mathrm{T}} R^{-1} v) \,\mathrm{d}t} \tag{40}$$

where P_0, Q, R and S are positive definite matrices that depend on the performance requirements. Because all the state equation matrices of equations (33) are continuous, the system ∞-norm $\|G_{err}\|_\infty$ is finite.[31] This means that there exists a positive scalar θ such that the optimal estimation $\hat{w}$ satisfies

$$\sup_{\varepsilon \neq 0} J_w \leqslant \frac{1}{\theta} \tag{41}$$

Conditions of the existence of a bound on the system ∞-norm $\|G_{err}\|_\infty$ and the lower bound of the ∞-norm can be derived using theorems given by Burl;[31] therefore the upper bound of θ can also be derived.[30] The derivation of the upper bound of θ is omitted because it is beyond the scope of this paper. The continuous-time H_∞ filter can be derived from equation (41) as

$$\dot{\hat{x}}_w = A_w \hat{x}_w + B_w u_m + P C_w^{\mathrm{T}} R^{-1}(y_m - C_w \hat{x}_w) \tag{42}$$

where

$$\hat{w} = L_w \hat{x}_w, \qquad \hat{x}_w(0) = \hat{x}_{w0}$$

and as

$$\begin{aligned}\dot{P} = {} & A_w P + P A_w^{\mathrm{T}} + E_w Q E_w^{\mathrm{T}}\\ & - P(C_w^{\mathrm{T}} R^{-1} C_w - \theta L_w^{\mathrm{T}} S L_w) P\end{aligned} \tag{43}$$

where

$$P(0) = P_0$$

and P is a symmetric positive definite matrix if the solution of equation (43) exists $\forall t \in [0, t_f]$. The detailed derivations of equations (42) and (43) can be found in the papers by Banavar and Speyer[28] and de Souza et al.[29] It is notable that the solution of the algebraic Riccati form of equation (43) can be used as

Table 1. Parameters of the test vehicle.

Symbol	Quantity	Value
m	Mass of the vehicle	1687 kg
I_z	Yaw moment of inertia	3401 kg m^2
L_f	Distance from the front axle to the centre of gravity	1.15 m
L_r	Distance from the rear axle to the centre of gravity	1.47 m
C_{f_ss}	Cornering stiffness of the front tyres	115,000 N/rad
C_{r_ss}	Cornering stiffness of the rear tyres	396,820 N/rad

P_0 in order to reduce the calculation complexity of equation (43) by taking the risk of increasing the estimation errors due to the initial state $x_w(0)$.[30] In this case, the steady-state H_∞ filter can be obtained from equations (42) and (43) as

$$\begin{aligned}\dot{\hat{x}}_w &= A_w\hat{x}_w + B_w u_m + P_0 C_w^{\mathrm{T}} R^{-1}(y_m - C_w\hat{x}_w)\\ &\quad A_w P_0 + P_0 A_w^{\mathrm{T}} + E_w Q E_w^{\mathrm{T}}\\ &\quad -P_0(C_w^{\mathrm{T}} R^{-1} C_w - \theta L_w^{\mathrm{T}} S L_w)P_0 = 0 \qquad (44)\end{aligned}$$

where

$$\hat{w} = L_w\hat{x}_w,\ \hat{x}_w(0) = (\,0 \quad 0 \quad 0\,)^{\mathrm{T}}$$

Since $w = \sin(\phi_b + \phi)$, the roll angle estimation ϕ is necessary in order to separate the road bank angle estimation from $\hat{w}$. The roll angle can be estimated using a vehicle-dynamics-based roll estimation method.[32]

Simulation results

Simulations were performed in order to verify the effectiveness and performance of the proposed estimation algorithm. A front-wheel-drive sport utility vehicle (SUV) model in CarSim® was selected as the vehicle model, and the proposed estimation algorithm was implemented by MATLAB®/Simulink® using the parameters shown in Table 1. The cornering stiffnesses C_{f_ss} and C_{r_ss} used for the estimator design were calculated by using the results of steady state cornering simulations and experiments. The lateral acceleration, the yaw rate and the longitudinal speed are assumed to be known in the simulations. These signals are normally available through the in-vehicle network of modern vehicles equipped with an electronic stability program (ESP).

In order to assess the performance and robustness of the proposed algorithm, the DFC method,[8] the UIO method[13,18] and the PIO method,[25,26] which do not require DGPS or any additional expensive sensors, were also implemented and simulated in this paper. The estimation parameters of the methods are carefully tuned to produce the best results. The estimation parameters for the UIO, the PIO and the PIF methods are decided by hand tuning processes based on the results of various simulations and experiments. The parameters identified through the processes are shown in Tables 2,3 and 4.

Table 2. Parameters of the UIO method.

Symbol	Quantity	Selected value
M_{uio}	Weight matrix for the outputs	$\begin{pmatrix} -10 & 10 \\ 10 & 10 \end{pmatrix}$
Q_{uio}	Weight matrix for E_{uio}	$\begin{pmatrix} 1 & 1 \\ 1 & 1 \end{pmatrix}$
τ_{uio}	Time constant of the filter	1/9

Table 3. Parameters of the PIO method.

Symbol	Quantity	Selected value
K_{po1}	Gain matrix for $\hat{x}_{po}$	$\begin{pmatrix} 1 & -\frac{v_x}{2} \\ 0 & -\frac{C_f L_f^2 + C_r L_r^2}{2 I_z v_x} \end{pmatrix}$
K_{po2}	Gain matrix for $\hat{w}_{po}$	$(\,0 \quad -2\,)$

Table 4. Parameters of the PIF method.

Symbol	Quantity	Selected value
Q	Weight matrix for the disturbances	0.1
R	Weight matrix for the noises	0.0035
S	Weight matrix for the estimation errors	1
P_0	Initial value of the Riccati equation	$\begin{pmatrix} 0 & 0 & 0 \\ 0 & 0 & 0 \\ 0 & 0 & 0.5 \end{pmatrix}$
θ	Parameter for the cost function	1

Straight road with a constant bank angle

Figure 2 shows simulation results when the vehicle travels on a straight road with a constant bank angle (30% = 16.7°). The vehicle was driven for 15 s with a constant longitudinal speed (80 km/h) and maintained a straight direction on the banked road. The purpose of this simulation is to compare the performance of the road bank angle estimation methods during steady state cornering on the banked road. Simulations were conducted for several different driving conditions with different types of modelling error and uncertainty in order to examine the robustness of the bank angle estimation methods. Figure 2(b) shows the simulation results when the driving condition is the same as the driving

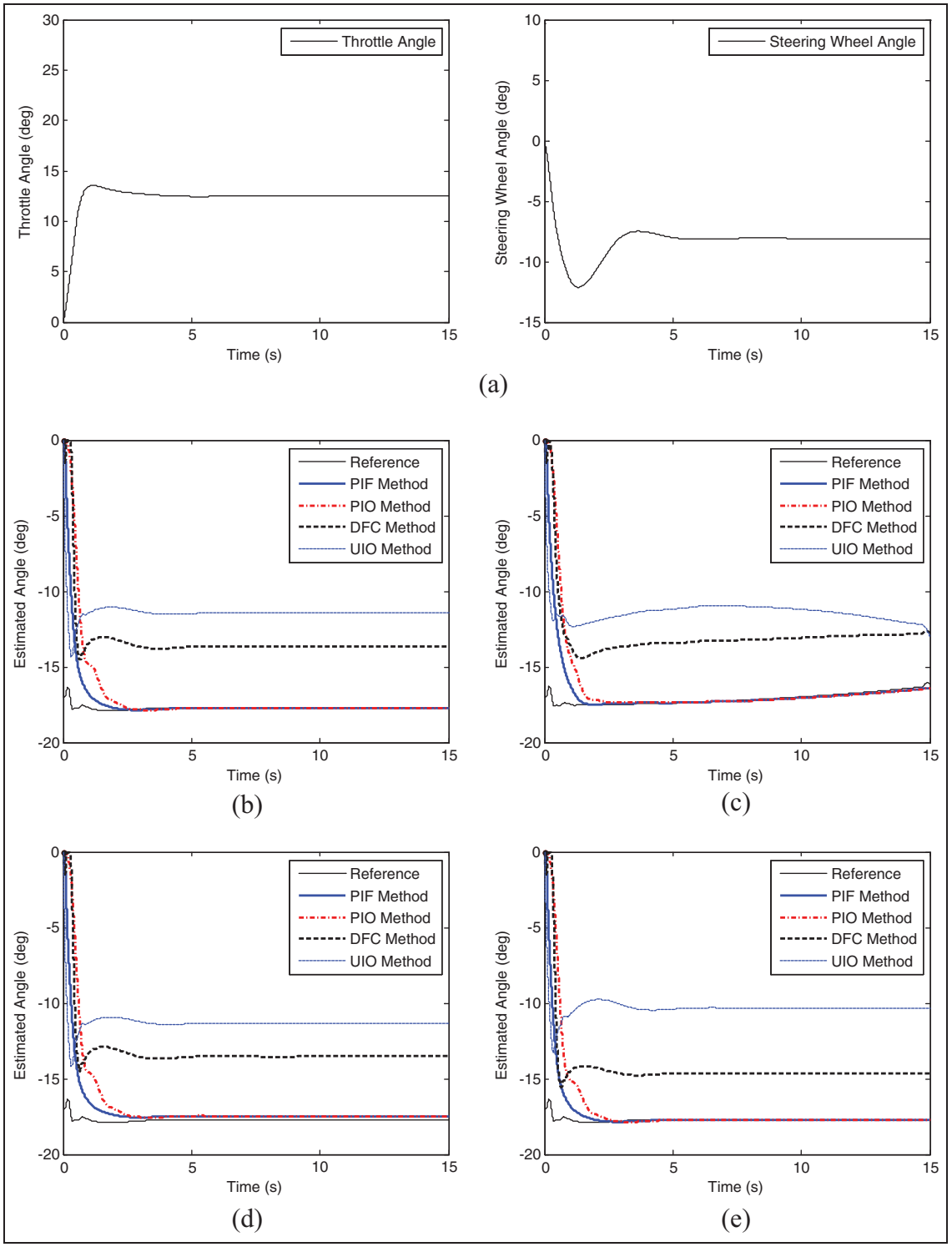

Figure 2. Simulation results (constant road bank angle): (a) driver inputs; (b) estimated φ ($\mu = 0.85$); (c) estimated φ ($\mu = 0.3$); (d) estimated φ ($a_y = a_{y\_real} \cos(10^\circ)$); (e) estimated φ ($C_f = 1.2C_{f\_ss}$).
PIF: proportional–integral H_∞ filter; PIO: proportional–integral observer; DFC: dynamic filter compensation; UIO: unknown input observer.

condition used for the estimation algorithm design. Figure 2(c) shows the simulation results when the road surface condition becomes more slippery (i.e. low μ). Figure 2(d) shows the simulation results when the lateral acceleration is measured incorrectly owing to the misaligned installation of the accelerometer and Figure 2(e) shows the simulation results when the actual cornering stiffness C_f is different from the cornering stiffness C_{f_ss} used for designing the estimation algorithm in Table 1, owing to the changes in the vehicle mass (e.g. more passengers). Simulation results were obtained by using the PIF method based on the modified vehicle

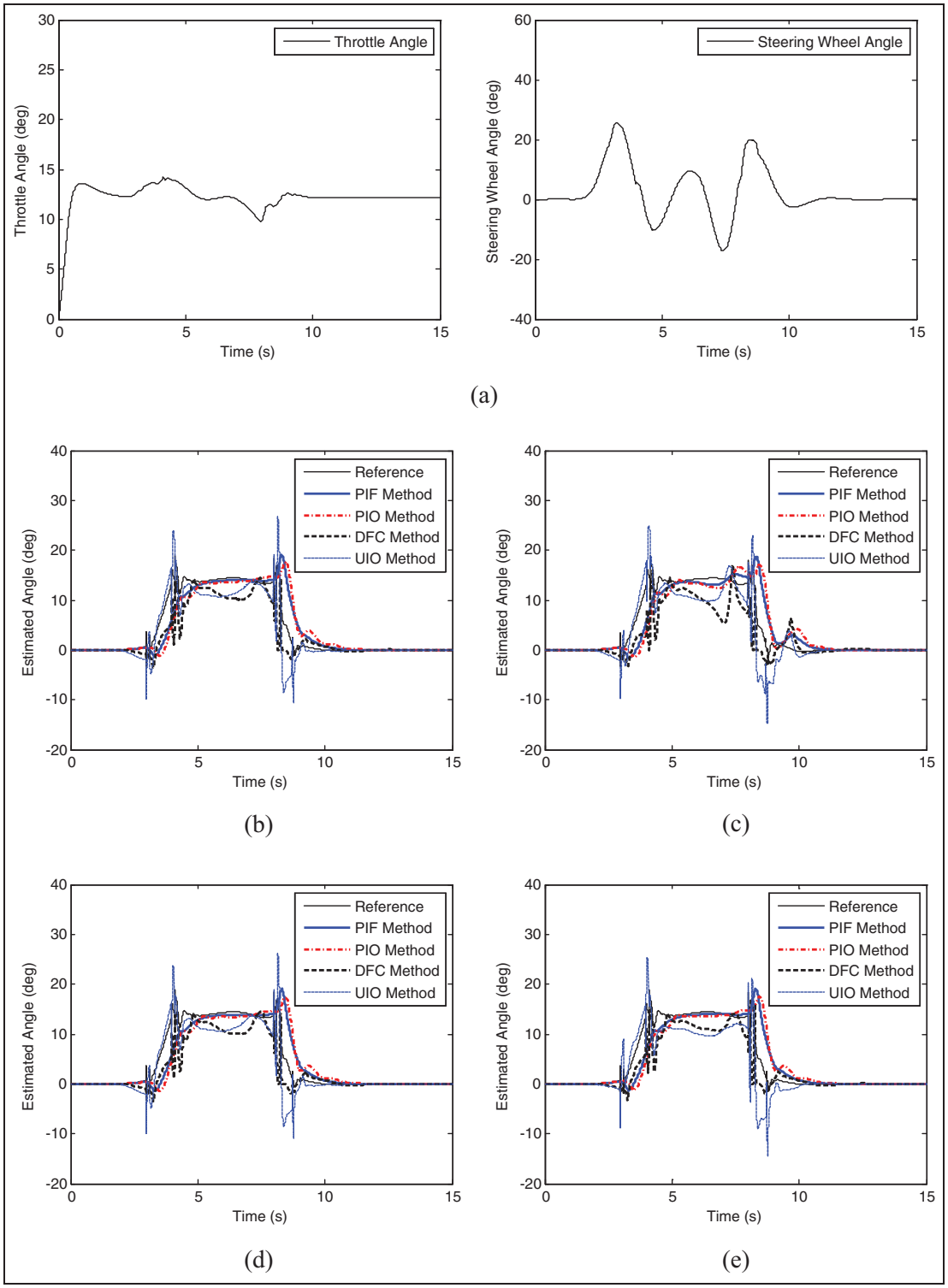

Figure 3. Simulation results (double lane change on a flat road): (a) driver inputs; (b) estimated φ ($\mu = 0.85$); (c) estimated φ ($\mu = 0.3$); (d) estimated φ ($a_y = a_{y\_real} \cos(10^\circ)$); (e) estimated φ ($C_f = 1.2C_{f\_ss}$).
PIF: proportional–integral H_∞ filter; PIO: proportional–integral observer; DFC: dynamic filter compensation; UIO: unknown input observer.

model, and by the PIO method, the DFC method and the UIO method based on the original model (4). The curves labelled Reference in Figure 2(b),(c),(d) and (e) are calculated as the difference between the absolute heights of the left and the right wheels provided by CarSim. As shown in the figures, because of the integral state in the observers, the PIF and the PIO methods yield better performances on estimating the bank angle without the steady state errors than the DFC and the UIO methods do.

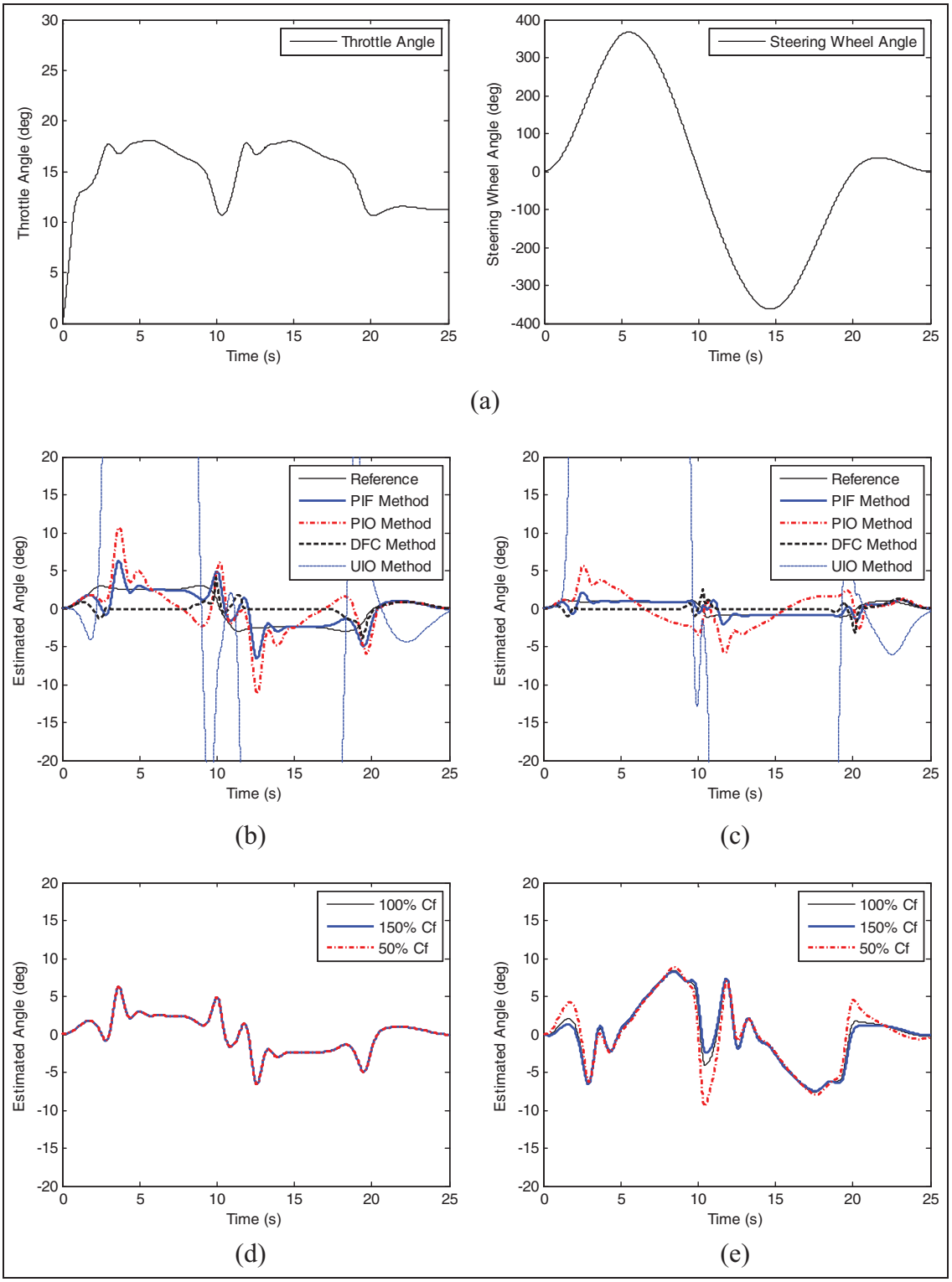

Figure 4. Simulation results (S-curve manoeuvre on a flat road): (a) driver inputs; (b) estimated φ ($\mu = 0.85$); (c) estimated φ ($\mu = 0.3$); (d) robustness of PIF with the modified vehicle model ($\mu = 0.85$); (e) robustness of PIF with the original vehicle model ($\mu = 0.85$).

PIF: proportional–integral H_∞ filter; PIO: proportional–integral observer; DFC: dynamic filter compensation; UIO: unknown input observer.

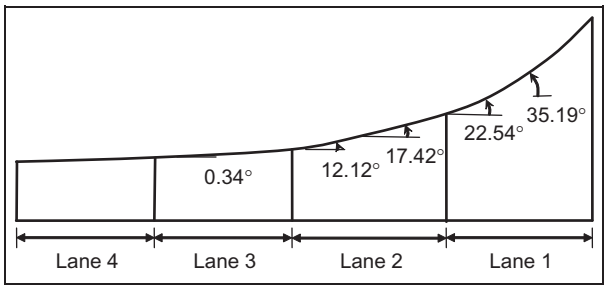

Figure 5. Test lanes and road bank angle status.

Bank angle change on a straight road

Figure 3 shows the simulation results when the vehicle travels on a straight road with two lanes, flat and banked (25% = 14°) lane, and changes lanes. Figure 3(a) shows the driving manoeuvre. The purpose of this simulation is to compare the performances of the road bank angle estimation methods when the road bank angle is changed. Similar to the constant-bank-angle case, simulations were conducted for several different driving conditions with different types of modelling error and uncertainty. The simulation results show that the modified-model-based PIF method yields the best performance and robustness in estimating the road bank angle and maintains its accuracy even in the presence of the model uncertainties.

S-curve manoeuvre on a flat road

Figure 4 shows the simulation results when the vehicle travels on a flat road during an S-curve manoeuvre ($\pm 360°$) at 60 km/h. The purpose of this simulation is to compare the values of the performance and robustness of the road bank angle estimation methods when the steering-wheel angle is large and the driving conditions are severe.

Figure 4(b) and (c) shows the estimation results of the reference, the PIF, the PIO, the DFC and the UIO methods. Among these, the PIF method shows the best estimation performance. Figure 3(d) and (e) shows simulation results when the actual cornering stiffness C_f differs from the cornering stiffness C_{f_ss} used for designing the estimation algorithm in Table 1 by 150% or 50% ($\mu = 0.85$). The results show that the PIF method based on the modified vehicle model yields better performance and robustness against the model uncertainties (C_f changes) than does the PIF method based on the original vehicle model.

Test validation

In order to verify the effectiveness and performance of the proposed method, vehicle tests were conducted under several different driving conditions. The test vehicle is an SUV equipped with an ESP and the test track is a high-speed circuit at the Korea Transportation Safety Authority. The ESP system contains several sensors, such as a yaw rate sensor (range, ± 100 deg/s; resolution, ± 0.3 deg/s; sensitivity, 18 mV/(deg/s)) and a lateral accelerometer (range, $\pm 1.8\,g$; resolution, $\pm 0.005\,g$; sensitivity, 1 V/g), which are also used in the bank angle estimation algorithm.

The test track consists of two straight courses and two cornering courses, and each course has four lanes, as shown in Figure 5. All the lanes are asphalt lanes and 16.2 m wide. Since the same vehicle is used in the simulations and vehicle tests, the same estimation algorithms and parameters used in the simulations are applied to the vehicle tests.

To mitigate the effect of the sensor noise on the road bank angle estimation, the reference bank angle and the bank angle estimation by the DFC method are filtered by a first-order low-pass filter (time constant, 2/3). The reference value of the bank angle is calculated from

$$\varphi_{reference} = \sin^{-1}\left(\frac{a_y - \dot{v}_y - v_x\dot{\psi}}{g}\right) \tag{45}$$

and assumed to be the actual bank angle in the test. The lateral acceleration $\dot{v}_y$ is calculated from the lateral velocity signal which is measured using a Corrsys SCE optical two-axis velocity sensor from Corrsys-Datron Co.

Straight driving on lane 1

Figure 6 shows the experimental results when the vehicle travels in lane 1, which is similar to the constant-steering-angle test in the simulation. As shown in Figure 6(a), the vehicle was driven for 15 s with a nearly constant longitudinal speed (about 143 km/h) and a nearly constant steering angle with only small adjustments. The results shown in Figure 6(b) and (c) are similar to the simulation results shown in Figure 3(b) and (e). The DFC and UIO methods cause steady state errors in Figure 6(b), and the errors are increased in Figure 6(c) owing to the model uncertainties regarding the cornering stiffness of the front tyres. Similar to the simulation results, the proposed PIF and PIO methods show good accuracy in the sense of the r.m.s. error and robustness against the model uncertainties.

Lane change between lanes 2 and 3

Figure 7 shows the experimental results when the vehicle travelled between lanes 2 and 3. As shown in Figure 7(a), the vehicle was driven for 25 s with several lane change manoeuvres. As shown in Figure 7(c) and (d), the proposed PIF with the modified vehicle model shows better robustness against the model uncertainties (C_f changes) than does the PIF with the original vehicle model.

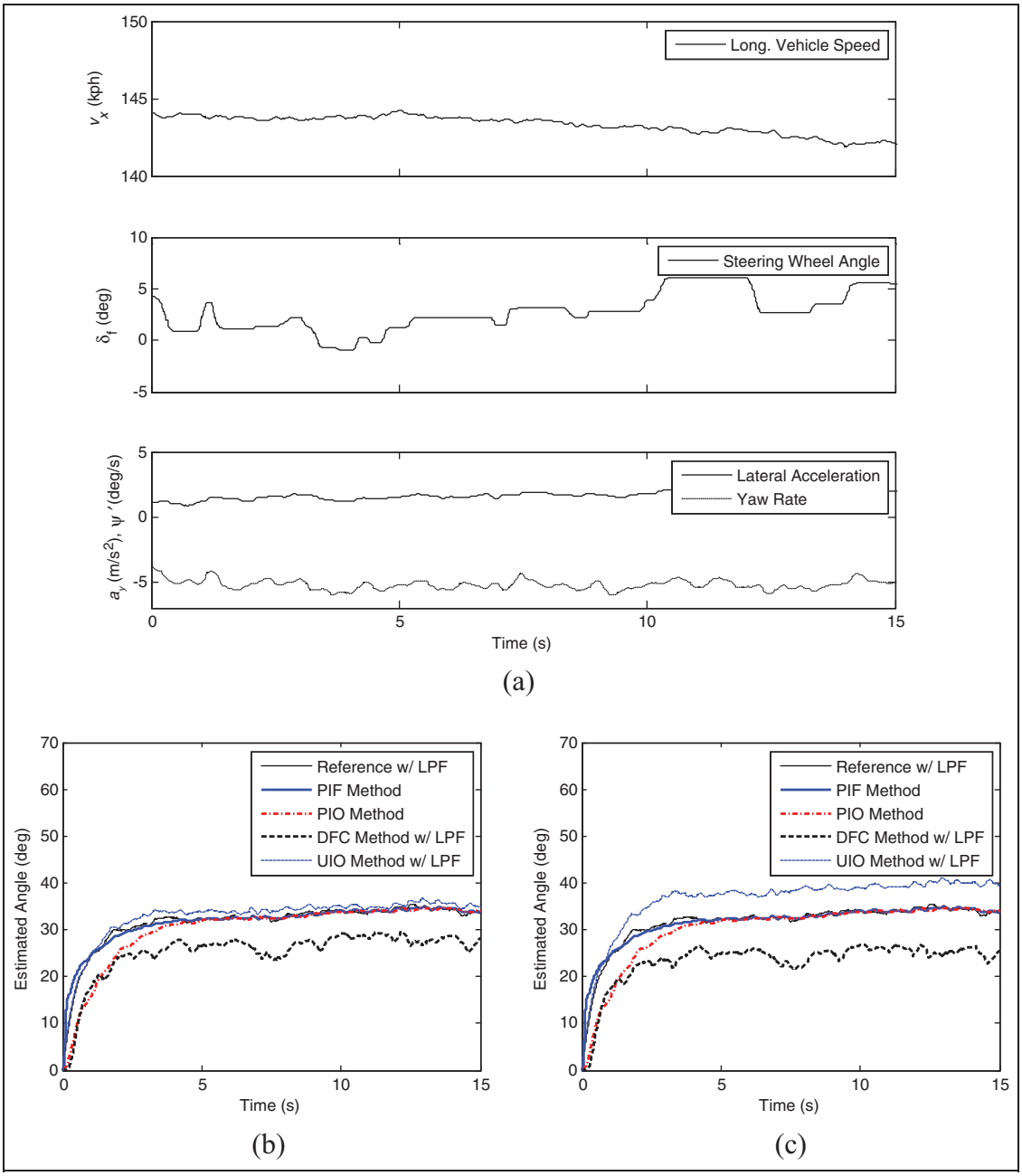

Figure 6. Test results (lane 1): (a) vehicle states from sensors; (b) estimated φ ($C_f = C_{f\_ss}$); (c) estimated φ ($C_f = 1.2C_{f\_ss}$).
Long.: longitudinal; w/ LPF: with a low-pass filter; PIF: proportional–integral H_∞ filter; PIO: proportional–integral observer; DFC: dynamic filter compensation; UIO: unknown input observer.

Conclusion

This paper presents a new robust road bank angle estimation method that is based on a PIF and does not require expensive sensors such as the DGPS. In this work, the robustness of the estimation was enforced by the use of a more robust system model and a robust estimation algorithm. A modified bicycle model, which reduces the model uncertainty by eliminating the lateral force term of the front tyre from the system equation, was derived and used to design a road bank angle estimation algorithm. A PIF based on the game theory approach, which is designed for the worst cases with respect to the sensor noises and disturbances, is used as the estimator in order to improve further the stability and robustness of the bank estimation. Simulations and actual vehicle tests are conducted for various road and vehicle driving conditions. The simulation and vehicle test results showed that the proposed PIF method provides the best accuracy and robustness against the model uncertainties compared with the previous methods, such as the DFC and the UIO methods.

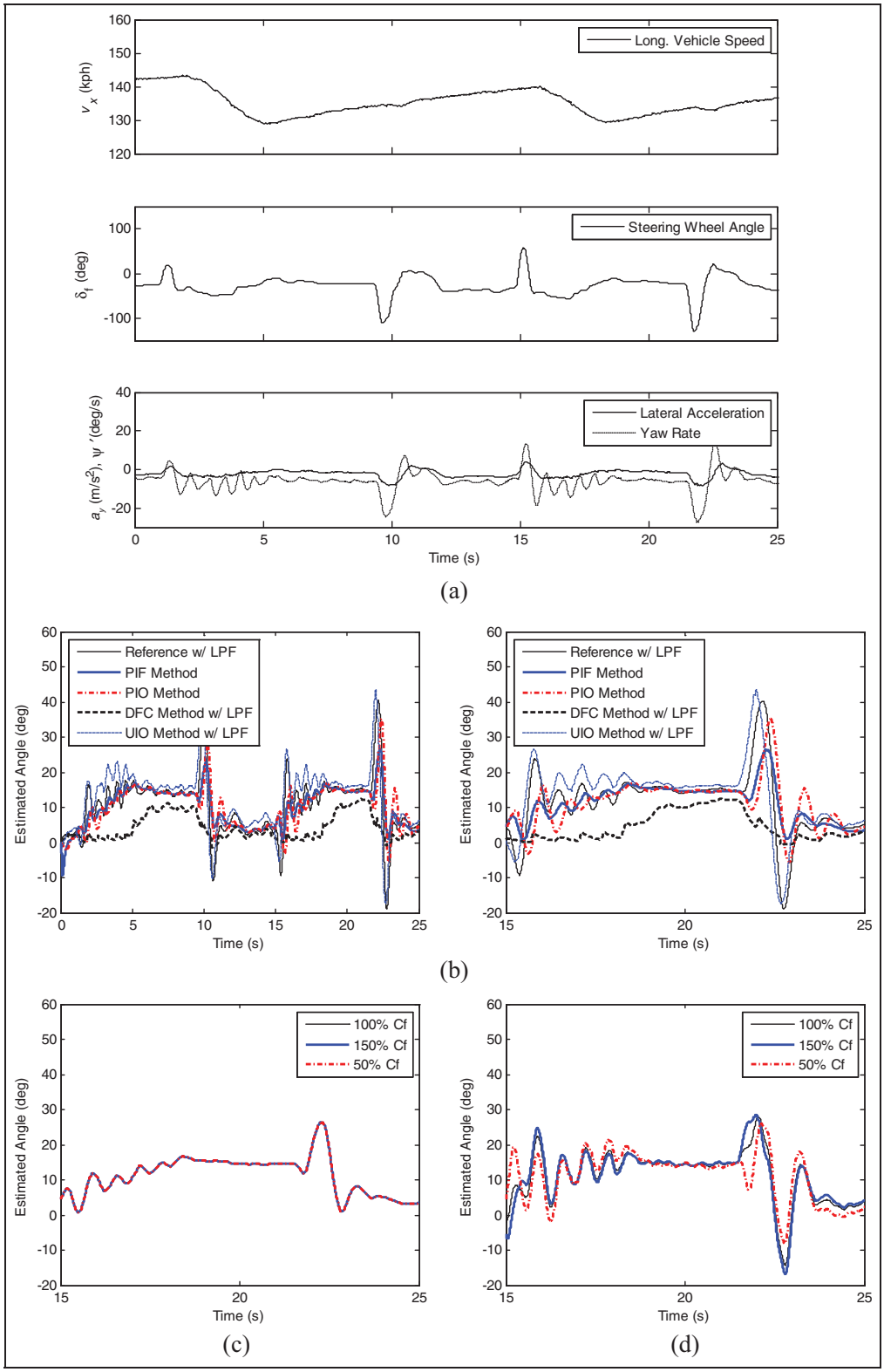

Figure 7. Test results (lane 2 ↔ lane 3): (a) vehicle states from sensors; (b) estimated φ; (c) robustness of PIF with the modified vehicle model; (d) robustness of PIF with the original vehicle model.

Long.: longitudinal; w/ LPF: with a low-pass filter; PIF: proportional–integral H_∞ filter; PIO: proportional–integral observer; DFC: dynamic filter compensation; UIO: unknown input observer.

Funding

This work was supported by Industry Source Foundation Establishment Project (grant no. 10037355) from the Korea Institute for Advancement of Technology, funded by the Ministry of Knowledge Economy, Republic of Korea, and the research fund of Hanyang University, Seoul, Republic of Korea.

References

1. Van Zanten AT, Erhardt R and Pfaff G. VDC, the vehicle dynamic control system of Bosch. SAE paper 950759, 1995.
2. Tseng HE, Ashrafi B, Madau D, et al. The development of vehicle stability control at Ford. *IEEE/ASME Trans Mechatronics* 1999; 4(3): 223–234.
3. Yoon J, Cho W, Koo B and Yi K. Unified chassis control for rollover prevention and lateral stability. *IEEE Trans Veh Technol* 2009; 58(2): 596–609.
4. Park J-I, Yoon J-Y, Kim D-S and Yi K-S. Roll state estimator for rollover mitigation control. *Proc IMechE Part D: J Automobile Engineering* 2008; 222(8): 1289–1311.
5. Cetin AE, Adli MA, Barkana DE and Kucuk H. Implementation and development of an adaptive steering-control system. *IEEE Trans Veh Technol* 2010; 59(1): 75–83.
6. Zheng B and Anwar S. Yaw stability control of a steer-by-wire equipped vehicle via active front wheel steering. *Mechatronics* 2009; 19(6): 799–804.
7. Sankaranarayanan V, Emekli ME, Guvenc BA, et al. Semiactive suspension control of a light commercial vehicle. *IEEE/ASME Trans Mechatronics* 2008; 13(5): 598–604.
8. Tseng HE. Dynamic estimation of road bank angle. *Veh System Dynamics* 2001; 36(4–5): 307–328.
9. Piyabongkarn D, Rajamani R, Grogg JA and Lew JY. Development and experimental evaluation of a slip angle estimator for vehicle stability control. *IEEE Trans Control Systems Technol* 2009; 17(1): 78–88.
10. Ryu J and Gerdes JC. Estimation of vehicle roll and road bank angle. In: *2004 American control conference*, Boston, MA, USA, 30 June–2 July 2004, vol 3, pp. 2110–2115. New York: IEEE.
11. Rajamani R, Piyabongkarn D, Tsourapas V and Lew JY. Real-time estimation of roll angle and CG height for active rollover prevention applications. In: *2009 American control conference*, St Louis, MO, USA, 10–12 June 2009, pp. 433–438. New York: IEEE.
12. Xu L and Tseng HE. Robust model-based fault detection for a roll stability control system. *IEEE Trans Control Systems Technol* 2007; 15(3): 519–528.
13. Mammer S, Glaser S and Netto M. Vehicle lateral dynamics estimation using unknown input proportional-integral observers. In: *2006 American control conference*, Minneapolis, MN, USA, 14–16 June 2006, pp. 4658–4663. New York: IEEE.
14. Hahn JO, Rajamani R, You SH and Lee KI. Real-time identification of road bank angle using differential GPS. *IEEE Trans Control Systems Technol* 2004; 12: 589–599.
15. Luczak S, Oleksiuk W and Bodnicki M. Sensing tilt with MEMS accelerometers. *IEEE Sensors J* 2006; 6(6): 1669–1675.
16. Fukada Y. Estimation of vehicle slip-angle with combination method of model observer and direct integration. In: *4th international symposium on advanced vehicle control*, Nagoya, Japan, 14–18 September 1998, pp. 375–388. Tokyo: JSAE.
17. Nishio A, Tozu K, Yamaguchi H, et al. Development of vehicle stability control system based on vehicle sideslip angle estimation. SAE paper 2001-01-0137, 2001.
18. Imsland L, Grip HF, Johansen TA and Fossen TI. On nonlinear unknown input observers – applied to lateral vehicle velocity estimation on banked roads. *Int J Control* 2006; 80(11): 1741–1750.
19. Hsu L-Y and Chen T-L. Estimating road angles with the knowledge of the vehicle yaw angle. *Trans ASME, J Dynamic Systems, Measmt, Control* 2010; 132(3): 31004.
20. Sebsadji Y, Glaser S and Mammar S. Vehicle roll and road bank angles estimation. In: *17th IFAC world congress*, Seoul, Republic of Korea, 6–11 July 2008, pp. 7091–7097. Oxford: Elsevier.
21. Grip HF, Imsland L, Johansen TA, et al. Estimation of road inclination and bank angle in automotive vehicles. In: *2009 American control conference*, St Louis, MO, USA, 10–12 June 2009, pp. 426–432. New York: IEEE.
22. Rajamani R. *Vehicle dynamics and control*. New York: Springer, 2005.
23. Jazar RN. *Vehicle dynamics: theory and applications*. New York: Springer, 2008.
24. Chen J and Patton RJ. *Robust model-based fault diagnosis for dynamic systems*. Norwell, MA: Kluwer, 1999.
25. Söffker D, Yu TJ and Müller PC. State estimation of dynamical systems with nonlinearities by using proportional–integral observer. *Int J Systems Sci* 1995; 26(9): 1571–1582.
26. Jiang G-P, Wang S-P and Song W-Z. Design of observer with integrators for linear systems with unknown input disturbances. *Electron Lett* 2000; 36(13): 1168–1169.
27. Marek J, Trah H-P, Suzuki Y and Yokomori I. *Sensors for automotive technology*. Weinheim: Wiley–VCH, 2003.
28. Banavar RN and Speyer JL. A linear-quadratic game approach to estimation and smoothing. In: *American control conference*, Boston, MA, USA, 26–28 June 1991, pp. 2818–2822. New York: IEEE.
29. de Souza CE, Shaked U and Fu M. Robust H_∞ filtering for continuous time varying uncertain systems with deterministic input signals. *IEEE Trans Signal Processing* 1995; 43(3): 709-719.
30. Simon D. *Optimal state estimation: Kalman, H_∞, and nonlinear approaches*. Hoboken, NJ: John Wiley, 2006.
31. Burl JB. *Linear optimal control*. Reading, MA: Addison Wesley Longman, 1999.
32. Kamnik R, Boettiger F and Hunt K. Roll dynamics and lateral load transfer estimation in articulated heavy freight vehicles: a simulation study. *Proc IMechE Part D: J Automobile Engineering* 2003; 217(11): 985–997.

Appendix

Notation

a_y	lateral acceleration of the vehicle (m/s^2)
A	state matrix
A_m	state matrix for the modified bicycle model
A_o	state matrix for the original bicycle model
A_w	state matrix for the bicycle model based on the proportional–integral observer

B	input matrix
C	output matrix
C_f	cornering stiffness of the front tyres (N/rad)
C_r	cornering stiffness of the rear tyres (N/rad)
D	input-to-output coupling matrix
e	estimation error
E	input matrix for the disturbance input
F_{yf}	front lateral force (N)
F_{yr}	rear lateral force (N)
g	acceleration due to gravity
G	transfer function matrix
h	distance from the centre of gravity to the roll centre (m)
H	transfer function
I	identity matrix
I_z	yaw moment of inertia of the vehicle (kg m^2)
J	cost function
K	gain matrix
K_{us}	understeer gradient of the vehicle
L	observer output matrix
L_f	distance from the front axle to the centre of gravity (m)
L_r	distance from the rear axle to the centre of gravity (m)
m	mass of the vehicle (kg)
M	weight matrix for the outputs
n	disturbance input for the bicycle model based on the proportional–integral observer
P	Riccati solution
Q	weight matrix for the disturbances
R	weight matrix for the noises
s	Laplace variable
S	weight matrix for the estimation errors
t	time (s)
t_f	final time (s)
u	system input
v	measurement noise
v_x	longitudinal speed of the vehicle (m/s)
v_y	lateral speed of the vehicle (m/s)
w	disturbance input
x	system state
$\hat{x}$	estimate of x
$x(0)$	initial state
$X(s)$	Laplace transform of x
y	system output
z	transformed state
α_f	front-tyre side-slip angle (rad)
α_r	rear-tyre side-slip angle (rad)
β	vehicle side-slip angle (rad)
β_f	global front-tyre sideslip angle (rad)
β_r	global rear-tyre sideslip angle (rad)
δ_f	steering-wheel angle (rad)
θ	parameter for the cost function
μ	tyre–road friction coefficient
ϕ	roll angle of the vehicle (rad)
ϕ_b	road bank angle (rad)
ψ	yaw angle of the vehicle (rad)